Online Junction Temperature Measurement of SiC-MOSFETs via Gate Impedance Using the Gate-Signal Injection Method

David Hirning, Luca Bauer, Johannes Ruthardt, Jörg Haarer, Philipp Ziegler, Jörg Roth-Stielow
INSTITUTE FOR POWER ELECTRONICS AND ELECTRICAL DRIVES
University of Stuttgart
Pfaffenwaldring 47
Stuttgart, Germany
Tel.: +49 / (711) – 685 67371
E-Mail: david.hirning@ilea.uni-stuttgart.de
URL: http://www.ilea.uni-stuttgart.de

Keywords

«TSEP», «Silicon Carbide (SiC)», «Reliability», «Junction Temperature Measurement»

Abstract

This paper presents a method for junction temperature monitoring of SiC-MOSFETs based on a high-frequency gate-signal injection. The signal is injected during steady state (e.g. off-state) resulting in a current response, which depends on the temperature dependent gate impedance. The external gate resistor is used as a current shunt to capture the current response. The resulting signal contains the junction temperature information due to the temperature dependency of the gate impedance. This paper focuses on a sinusoidal approach to overcome the challenges due to the temperature dependent parasitic capacitance of the gate circuit. Measurements show the proof of concept, however, there are still challenges to face.

Introduction

In recent years, there has been a trend in power electronics towards more compact and faster switching designs. This development was made possible by constantly improved and partly new types of power transistors. Due to this trend power transistors are also facing new challenges. As a result of the higher switching frequencies and the higher integration level, the thermal stress of the power transistors is increasing.

In order to counteract this and increase the reliability, a high dynamic junction temperature measurement creates the possibility of detecting over temperature and an online health monitoring [1] or even temperature control [2, 3, 4].

The gate-signal injection method has been successfully implemented and investigated for Si-IGBTs [1, 5–9]. Applying this method to SiC-MOSFETs is more complex due to the temperature dependent parasitic capacitance of the gate circuit, by which a sign change of the sensitivity of the temperature dependent impedance of the gate circuit can appear, as shown in [10, 11]. Through a sign change in the sensitivity an ambiguous relationship between the temperature and the gate impedance can occur, which makes it impossible to infer the temperature from the impedance [10]. Because the sensitivity as well as the impedance is strongly dependent on the frequency, a simplified rectangular signal injection can have a negative influence on the temperature measurement due to its harmonics at higher frequencies, as described in [10]. This is why in this paper a more complex sinusoidal approach is selected, similar to the approach described in [7] for Si-IGBTs. It is investigated how the sinusoidal approach can improve the accuracy of the measurement.

This paper presents a gate-signal injection method, which overcomes the challenges due to the temperature dependent parasitic capacitance of the gate circuit, which will be validated by measurements.

Approach

Fig. 1 (left) shows a simplified circuit of the gate-driver circuit of the SiC-MOSFET. The voltage v_dr is the voltage applied by the gate driver, R_G is the external gate resistor, L_P the parasitic inductance of the MOSFET as well as of the gate-driver circuit, R_Gi the temperature dependent internal gate resistance and C_P the parasitic temperature dependent input capacitance of the MOSFET [10, 12, 12]. Due to the temperature dependent elements within the gate-driver circuit the impedance $\underline{Z}_G$ of the gate-driver circuit is temperature dependent as well, see (1).

$$\underline{Z}_\mathrm{G}(\omega_\mathrm{I}, T_\mathrm{j}) = R_\mathrm{G} + R_\mathrm{Gi}(T_\mathrm{j}) + j\omega_\mathrm{I} L_\mathrm{P} + \frac{1}{j\omega_\mathrm{I} C_\mathrm{P}(T_\mathrm{j})} \tag{1}$$

Since the temperature dependency cannot be measured directly, a high frequency sinusoidal signal is injected into the gate circuit, while the MOSFET is in off-state, see Fig. 1 (right) [8]. Due to the injection the operation of the MOSFET is limited, because the time in off-state of the MOSFET t_off needs to be at least as long as the injection takes place. The injected signal has the frequency ω_I and the amplitude v_i. This signal causes a gate current which again leads to a voltage drop across the external gate resistor. By means of a voltage divider, as seen in equation (2), the voltage drop across the external gate resistor is described as a function of the frequency of the injected signal as well as of the junction temperature [1, 7, 8].

$$v_\mathrm{RG} = v_\mathrm{i} \cdot \frac{R_\mathrm{G}}{\left|\underline{Z}_\mathrm{G}(\omega_\mathrm{I}, T_\mathrm{j})\right|} \tag{2}$$

If the relationship between the temperature and the voltage drop across the external gate resistor is biunique, the junction temperature can be inferred by the voltage drop across the external gate resistor [10], hence it is mandatory to find a frequency of the injected signal, at which this relationship is biunique.

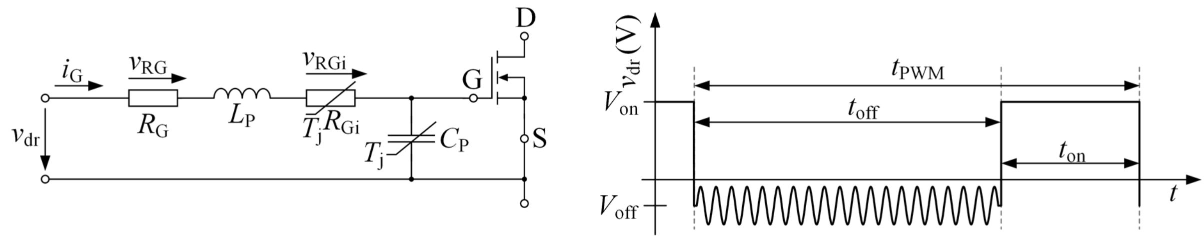

Fig. 1: Equivalent circuit diagram of the gate-driver circuit (left). Gate-driver voltage v_dr (right)

Furthermore the sensitivity, which is the derivative of the voltage drop across the external gate resistor with respect to the temperature, see (3), should be as high as possible for a precise and robust measurement [1, 7, 8].

$$s_\mathrm{V} = \frac{\mathrm{d}v_\mathrm{RG}}{\mathrm{d}T_\mathrm{j}} = \frac{\mathrm{d}}{\mathrm{d}T_\mathrm{j}} v_\mathrm{i} \cdot \frac{R_\mathrm{G}}{\left|\underline{Z}_\mathrm{G}(\omega_{\mathrm{I},} T_\mathrm{j})\right|} \tag{3}$$

Hence a frequency not only with a biunique relationship, but also with the highest possible sensitivity should be selected [10]. Therefor a profound investigation of the gate circuit of the SiC-MOSFET is mandatory.

Investigations of the gate circuit

To find a frequency, matching the requirements, a half-bridge SiC-module (BSM120D12P2C005 by Rohm) is investigated with a network analyzer (Bode100, Omicron). For the investigations, only the low side of the module is considered, since the test setup is a buck converter, which only uses the low side MOSFET. The MOSFET is investigated within a gate-driver circuit as in Fig. 1 (left).

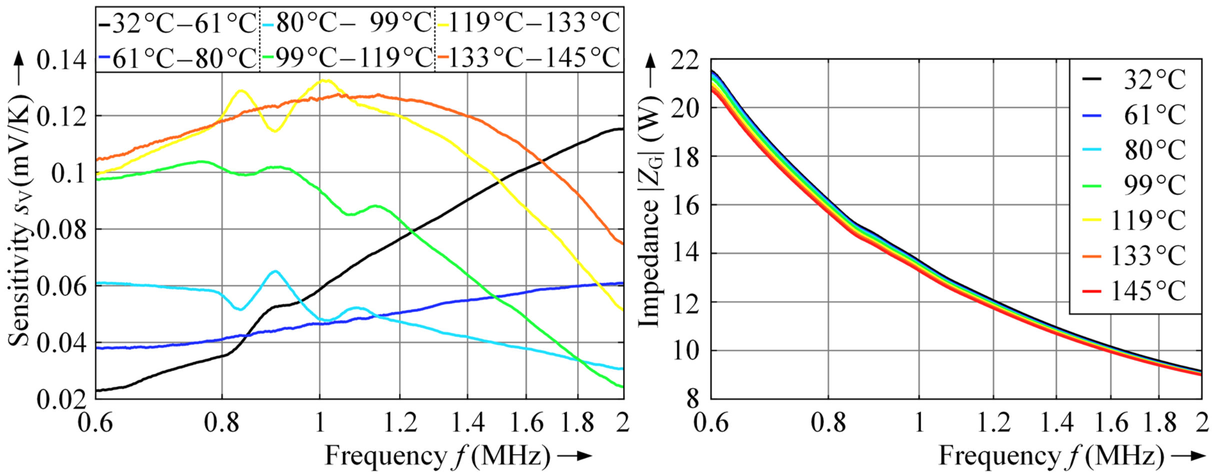

Fig. 2: Sensitivity of the voltage drop across the external gate resistor depending on the frequency (left). Temperature dependency of the impedance of the gate driver circuit depending on the frequency (right).

As already mentioned, a biunique relationship between the voltage drop and the temperature is mandatory, thus the sensitivity s_v must not change its sign over the target temperature range at the preferred frequency. Fig. 2 shows the sensitivity s_v as well as the absolute value of the impedance $\underline{Z}_G$ depending on the temperature and the frequency. It can be seen, that the impedance decreases with increasing temperature within the depicted frequency range. Furthermore, the temperature dependency of the impedance is biunique for the shown frequencies, which can also be seen within the sensitivity, because the sensitivity does not change its sign in this frequency range. The sensitivity s_v of the voltage drop across the external gate resistor is calculated by differentiation with respect to the junction temperature and the parameters from Tab. I, as seen in (3). The voltage V_{DS} is set to $V_{DS} = 30$ V, since the change of the input capacitance of the MOSFET is neglectable above a drain-source voltage of $V_{DS} = 10$ V [13]. Because the measurement is not continuous, the difference quotient of the measured data is used, see (4).

$$s_v = \frac{\mathrm{d}v_{RG}}{\mathrm{d}T_j} \approx \frac{\Delta v_{RG}}{\Delta T_j} = \frac{\Delta}{\Delta T_j} v_i \cdot \frac{R_G}{\left|Z_G(\omega_i, T_j)\right|} \tag{4}$$

Table I: Parameters of the impedance measurement and for the calculation of the sensitivity

Parameter	**Value**
V_{GS}	-5 V
V_{DS}	30 V
T_j	32°C – 145°C
f_i	0.6 MHz – 1 MHz
R_G	5.6 Ω

The sensitivity varies strongly with the temperature and the frequency. For higher temperatures the sensitivity has its maximum between 1 MHz and 1.2 MHz. For temperatures in the middle range the sensitivity decreases with an increasing frequency. In contrast to this the sensitivity increases with increasing frequency for lower temperatures. Depending on the field of application a frequency can be selected with the optimal sensitivity. To find a frequency with the best results over the whole temperature range the voltage difference Δv_{RG}, see (5), between the lowest and highest temperature is considered, see Fig. 3. The voltage difference has its maximum between 1 MHz and 1.2 MHz, so the linearized sensitivity over the whole temperature range has its optimum within these frequencies.

$$\Delta v_{RG} = v_{RG}(145°C) - v_{RG}(32°C) \tag{5}$$

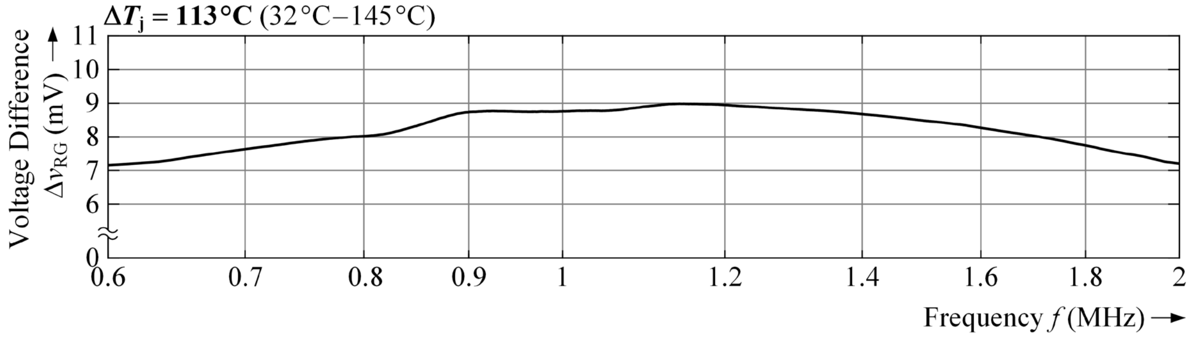

Fig. 3: Change in voltage depending on the frequency over the complete temperature range from 32°C to 145 °C.

Realization

The superimposed sinusoidal signal v_i is provided by a signal generator and is superimposed by means of a transformer, as seen in Fig. 4. The capacitance C_d decouples the injection path from the DC-voltage. To turn off the MOSFET a current can flow through the diodes D_1 and D_2, but the added forward voltage of the diodes is high enough to block the injected signal. Without the added forward voltage the injected signal would be shorted. The voltage $v_{off,i}$ is the sum of the turn off voltage v_{off} and the injected voltage v_i as seen in Fig. 1 (right).

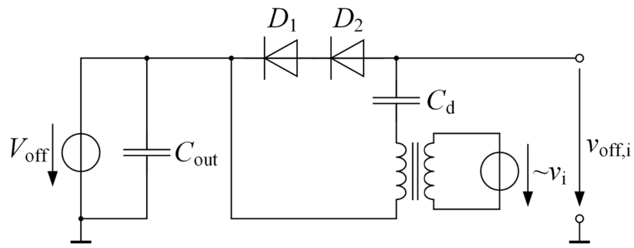

Fig. 4: Signal injection circuit

The voltage $v_{off,i}$ is connected to the driver IC, which again applies this voltage into the gate-driver circuit, see Fig. 5 (left). For the measurement of the voltage drop across the external gate resistor a differential amplifier is used. Fig. 5 (right) shows the measurement circuit as well as the signal processing of the measured voltage. By means of an IC the RMS value of the voltage drop across the external gate resistor is formed. This signal again is filtered, amplified and adjusted to the input voltage range of an analog-digital converter, which is read out by a microcontroller, where the calibration curve is lodged, to infer to the junction temperature [7]. The value of the voltage v_{ADC} is converted every PWM cycle.

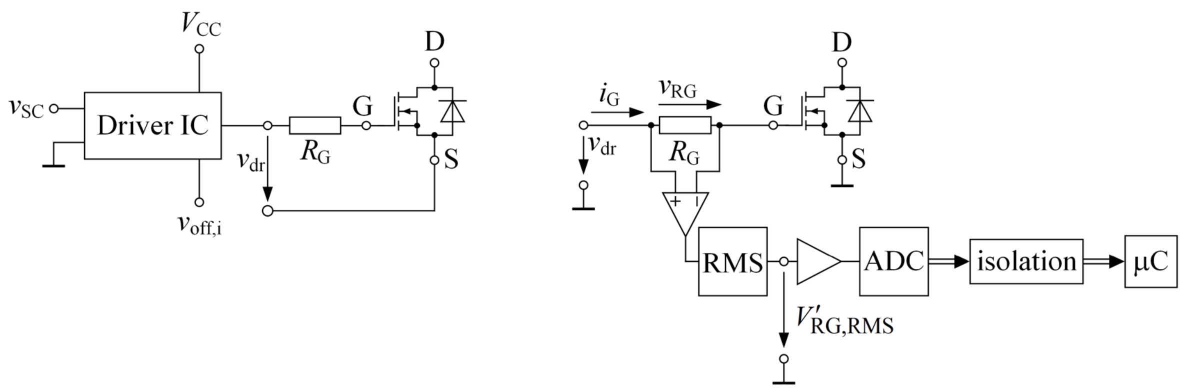

Fig. 5: Gate-driver circuit with driver IC (left). Signal processing of the measured voltage drop across the external gate resistor (right).

Fig. 6 shows the gate-driver voltage v_{dr}, the RMS-value $V`_{RG,RMS}$ of the voltage across the external gate resistor as well as the input voltage v_{ADC} of the analog-digital converter, during operation of the MOSFET with no drain-source voltage applied. Looking at the gate-driver voltage, the superimposed sinusoidal signal can be seen while the MOSFET is in off-state. The injected signal has a frequency f_i of f_i = 1 MHz. The RMS-value of the voltage drop is filtered by a second-order low pass filter to minimize noise. Due to the low sensitivity and the small change in voltage over the entire temperature range, as seen in Fig. 2 and 3, the RMS-value has to be highly amplified. The RMS-value can be seen in Fig. 6, it seems to be in steady state at about 20 µs. But in the amplified and adjusted voltage v_{ADC}, it is clear to see, that the voltage signal is still in its transient response. Even at the end of the signal injection the voltage signal is not in steady state. Since the voltage v_{ADC} is converted each PWM-cycle at the same time this will be neglected for the measurements.

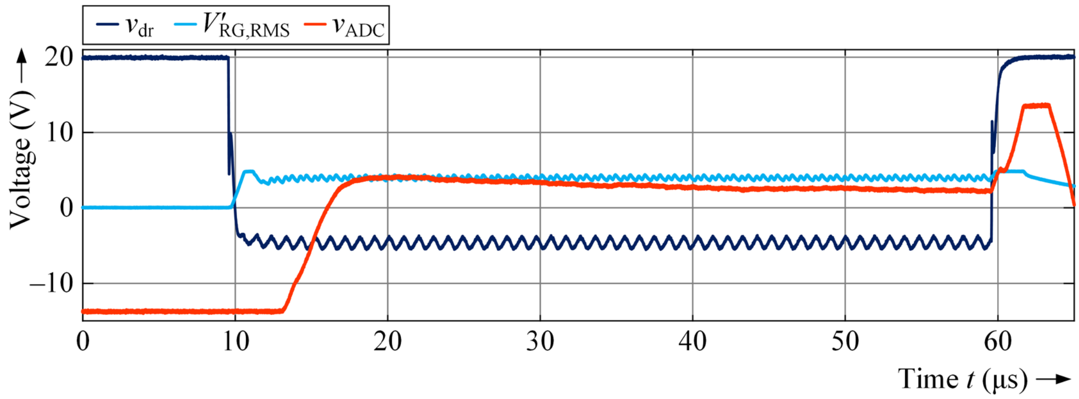

Fig. 6: Gate-driver voltage, measured RMS-value of the voltage drop and the filtered and amplified RMS-value before the analog-digital converter.

Measurements

In a first experiment the MOSFET was heated twice with a heat gun. A significant change in the voltage drop across the external gate resistor occurred, see Fig. 7. The heating and cooling phase of the MOSFET can be clearly seen. The MOSFET is mounted to a heat sink. Furthermore, the presented measurement principle is investigated in an operating test setup as seen in Fig. 8.

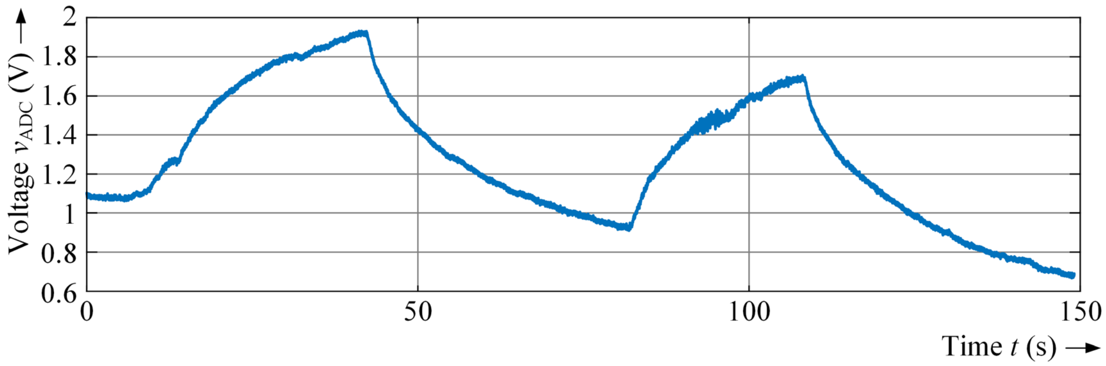

Fig. 7: Measured voltage across the external gate resistor while heating the MOSFET with a heat gun twice.

The MOSFET is used in a buck converter with an ohmic-inductive load. The temperature is monitored with an infrared camera as a reference to the gate-signal injection method. Therefore, the SiC-module is opened and blackened so the infrared camera captures the junction temperature as precise as possible [8]. The parameters of the test setup can be found in Tab. II.

To infer to the junction temperature a calibration must be executed. Due to the high frequency signal injection the range of adjustment of the duty cycle is limited. Since the injection period is set to t_i = 50 µs the maximum settable duty cycle is 50 %. For the calibration this duty cycle is set and the MOSFET is heated. While heating the MOSFET the voltage across the external gate resistor as well as the junction temperature captured by the infrared camera is recorded, see Fig. 9. The calibration curve, Fig. 9, shows a biunique relationship between the junction temperature and the converted voltage across the external gate resistor from 40°C to about 105°C. Within this temperature range it is possible to infer to the junction temperature by means of the calibration curve. For temperatures above 105°C the voltage v_{ADC} no longer increases with increasing temperature, so the relationship is no longer biunique. The investigations of the gate-driver circuit (Fig. 2) showed a biunique relationship for temperatures until 145°C, however, this behavior cannot be verified within the calibration. An assumption for this is a temperature drift within the signal processing of the measured voltage drop across the external gate resistor, which could be neglected by a differential measurement approach. This has to be further investigated.

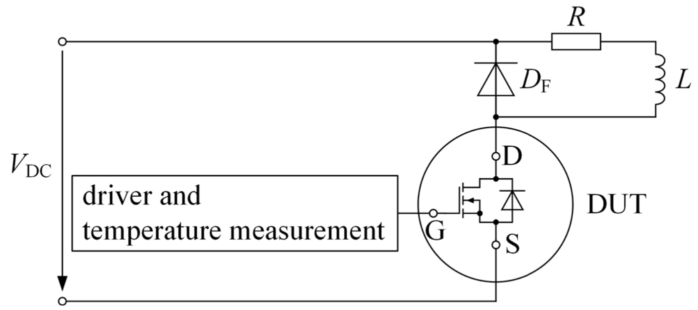

Fig. 8: Test setup of the junction temperature measurement.

Table II: Parameters of the test setup.

Parameter	**Value**
R	1.5 Ω
L	610 µH
V_{DC}	215 V
f_{PWM}	10 kHz
f_i	1 MHz
R_G	5 Ω

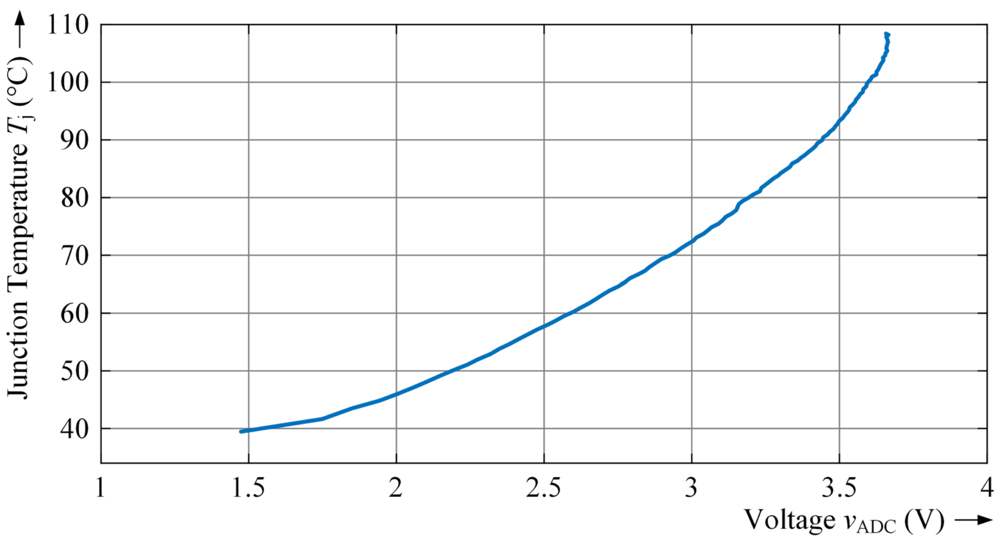

Fig. 9: Calibration curve.

In a first measurement the test setup is operated in the same operation point as for the calibration curve. The duty cycle is set to 50%, the result is depicted in Fig. 10. In the first plot in blue the by means of the gate-signal injection method inferred junction temperature and in red the reference temperature from the infrared camera is shown. In the second plot the deviation between the reference and the TSEP-method can be seen. The deviation is throughout the whole measurement range less than 2 K, so in this operation point the presented signal injection method provides good results.

$$\Delta T_j = T_{j,\text{reference}} - T_{j,\text{TSEP-method}} \tag{6}$$

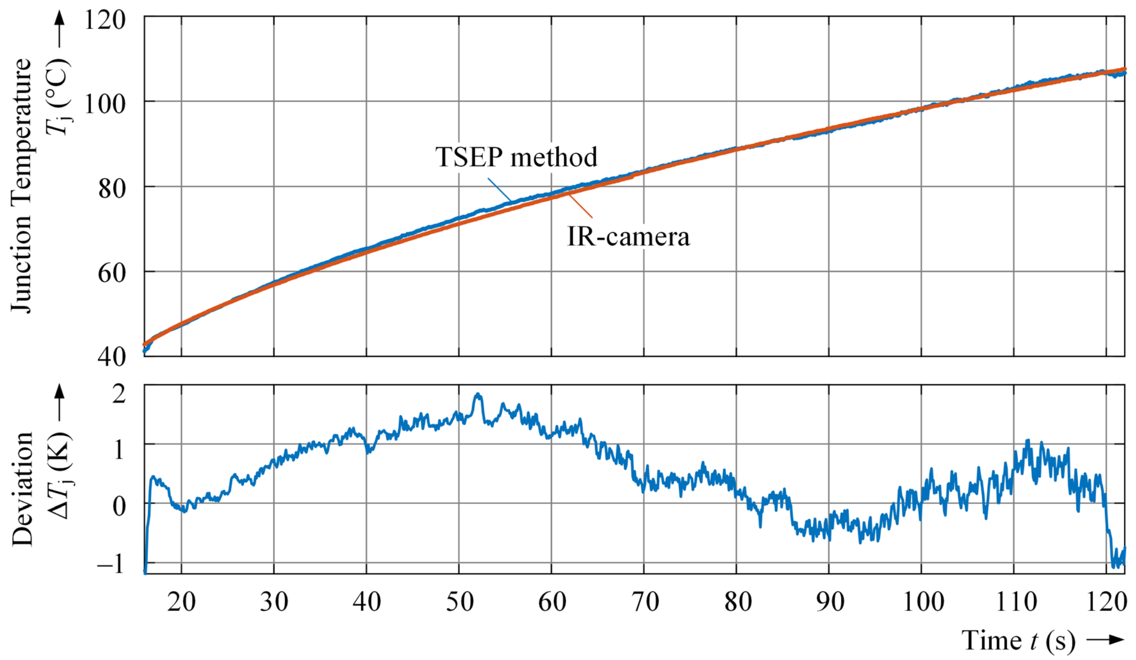

Fig. 10: Inferred and reference junction temperature for a duty cycle of 50% (top) and deviation from the reverence temperature (bottom).

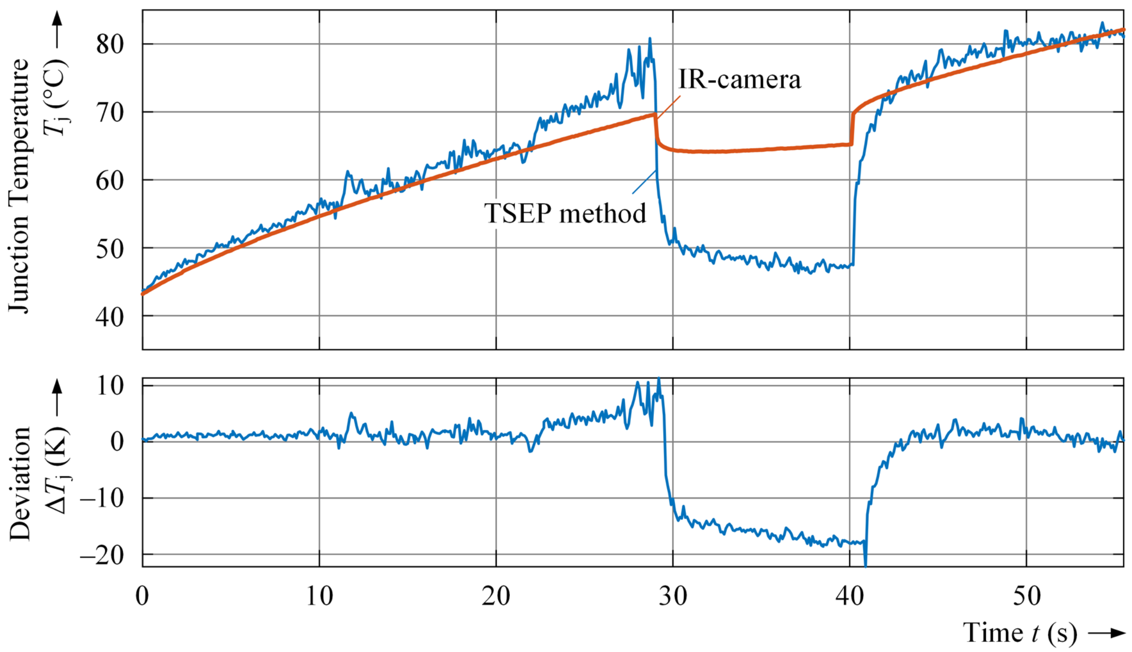

Fig. 11: Inferred and reference junction temperature for different duty cycles (50%, 35%, 50%) (top) and deviation from the reverence temperature (bottom).

In a second measurement, Fig. 11, the duty cycle is varied. In the first interval the duty cycle is set to 50% as in the calibration until about t = 29 s. In the second interval the duty cycle is set to 35% for about 11s and in the third and last interval the duty cycle is set to 50% until the end of the measurement. For both intervals with a duty cycle of 50% the deviation is less than 10 K, most of the time even less than 5 K. As seen in the first measurement the method provides good results within the operation point of the calibration. For the second interval the deviation is up to 20 K, it can be seen, that the method, implemented as presented, only provides usable results within the operation point of the calibration. By varying the duty cycle, respectively the load current, the inferred temperature deviates highly from the actual junction temperature. However, these measurements provide a general proof of concept, but for an actual usage of the presented method further investigations have to be made.

Conclusion

This paper presents a junction temperature measurement setup for the gate-signal injection method using a high frequent sinusoidal signal to overcome the challenge due to the temperature dependent parasitic capacitance of the gate circuit. An investigation on the gate-driver circuit of the MOSFET shows, that a junction temperature measurement via the temperature dependent gate impedance is possible. Therefore, a signal injection circuit as well as a measurement circuit is shown. This setup is tested in an initial experiment with a heat gun and shows promising results. For further validation a test setup is introduced and within this setup measurements are performed. The high frequency gate-signal injection method provides good results within the electric operation point of the calibration. However, for other operation points there is a high deviation between the actual junction temperature and the junction temperature inferred by means of the presented TSEP-method. For an actual usage of the presented method further investigations have to be made.

References

[1] M. Denk, "In-Situ-Zustandsüberwachung von IGBT-Leistungshalbleitern mittels Echtzeit-Sperrschichttemperaturmessung," 2016. [Online]. Available: https://eref.uni-bayreuth.de/32289/

[2] Ruthardt Johannes, Schulte Hendrik, Ziegler Philipp, Fischer Manuel, Nitzsche Maximilian, and Roth-Stielow Jörg, "Junction Temperature Control Strategy for Lifetime Extension of Power Semiconductor Devices," in *2020 22nd European Conference on Power Electronics and Applications (EPE'20 ECCE Europe)*, 2020, pp. 1–9.

[3] J. Ruthardt *et al.,* "Closed Loop Junction Temperature Control of Power Transistors for Lifetime Extension," in *2020 IEEE Applied Power Electronics Conference and Exposition (APEC)*, 2020, p. 2955.

[4] van der Broeck Christoph H., Polom Timothy A., Lorenz Robert D., and De Doncker Rik W., "Real-Time Monitoring of Thermal Response and Life-Time Varying Parameters in Power Modules," *IEEE Transactions on Industry Applications*, vol. 56, no. 5, pp. 5279–5291, 2020, doi: 10.1109/TIA.2020.3001524.

[5] Denk Marco and Bakran Mark-M., "Junction Temperature Measurement during Inverter Operation using a TJ-IGBT-Driver," in *Proceedings of PCIM Europe 2015; International Exhibition and Conference for Power Electronics, Intelligent Motion, Renewable Energy and Energy Management*, 2015, pp. 1–8.

[6] Denk Marco and Bakran Mark-M., "Comparison of UCE- and RGi-based junction temperature measurement of multichip IGBT power modules," in *2015 17th European Conference on Power Electronics and Applications (EPE'15 ECCE-Europe)*, 2015, pp. 1–11.

[7] Denk Marco and Bakran Mark-M., "An IGBT Driver Concept with Integrated Real-Time Junction Temperature Measurement," in *PCIM Europe 2014; International Exhibition and Conference for Power Electronics, Intelligent Motion, Renewable Energy and Energy Management*, 2014, pp. 1–8.

[8] Ruthardt Johannes *et al.,* "Online Junction Temperature Measurement via Internal Gate Resistance Using the High Frequency Gate Signal Injection Method," in *PCIM Europe 2019; International Exhibition and Conference for Power Electronics, Intelligent Motion, Renewable Energy and Energy Management*, 2019, pp. 1–7.

[9] Denk Marco and Bakran Mark-M., "IGBT Gate Driver with Accurate Measurement of Junction Temperature and Inverter Output Current," in *PCIM Europe 2017; International Exhibition and Conference for Power Electronics, Intelligent Motion, Renewable Energy and Energy Management*, 2017, pp. 1–8.

[10] J. Ruthardt *et al.,* "Investigations on Online Junction Temperature Measurement for SiC-MOSFETs Using the Gate-Signal Injection Method," in *2021 IEEE Energy Conversion Congress and Exposition (ECCE)*, 2021, pp. 5354–5359.

[11] T. Kestler and M.-M. Bakran, "Expansion of the Junction Temperature Measurement via the Internal Gate Resistance to a wide range of Power Semiconductors," in *2019 21st European Conference on Power Electronics and Applications (EPE '19 ECCE Europe)*, 2019, pp. 1–9.

[12] S. M. Sze, *Physics of semiconductor devices,* 3rd ed. Hoboken, N.J: Wiley-Interscience, 2007.
[13] Rohm Co., Ltd., *SiC Power Module BSM120D12P2C005 Datasheet.* [Online]. Available: https://fscdn.rohm.com/en/products/databook/datasheet/discrete/sic/power_module/bsm120d12p2c005-e.pdf